CrossMark

ORIGINAL PAPER

Fabrication and characterization of electrospun PVA/CdS and PVA/TiO$_2$ nanocomposite thin films as n-type semiconductors

P. Ferdowsi[1] · J. Mokhtari[1]

© Springer-Verlag Berlin Heidelberg 2015

Abstract Poly(vinyl alcohol) (PVA)/CdS and PVA/TiO$_2$ nanocomposite thin films were prepared at different semiconductor nanoparticles ratio (20, 30, 40 and 50 CC) by employing electrospinning method. For the former, CdS nanoparticles were first synthesized using cadmium nitrate (Cd (NO$_3$)$_2$) and sodium sulfide (Na$_2$S) in a simple and economical way whereas for the latter, TiO$_2$ was purchased. Morphology and structure of nanocomposites were characterized by X-ray diffraction (XRD) and scanning electron microscope. The results indicated the cubic and anatase structure of CdS and TiO$_2$ nanoparticles in PVA matrix, respectively, and proved that nanoparticles were successfully coated by PVA molecules. Optical properties of samples were also characterized by diffuse reflectance spectroscopy. Particle sizes of CdS and TiO$_2$, <9 and 15 nm, respectively, were calculated with the results obtained from XRD observation and it was found to be in agreement with the absorption spectra of both nanocomposites. The prepared films at 50:50 ratio, in both PVA/CdS and PVA/TiO$_2$, were found to be suitable for application in solar cell as a window layer due to the crystalline phase, favorable band gap (2.53, 3.31 eV) and higher optical transmittance.

Keywords PVA/CdS · PVA/TiO$_2$ · Nanocomposite · Electrospinning · Optical properties

✉ J. Mokhtari
  j.mokhtari@guilan.ac.ir

[1] Department of Textile Engineering, Faculty of Engineering, University of Guilan,
    41635-3756 Rasht, Iran

Introduction

In recent years, preparation of semiconductor nanocrystalline thin films has gained a great deal of attention for their unique size-dependent properties and potential applications in solar cells [1, 2], light emitting diodes (LED) [3], nonlinear optical devices [4], semiconductor lasers [5] and fiber filter [6]. Cadmium sulfide (CdS) and titanium dioxide (TiO$_2$) are two of the most important semiconductors which are used as a window layer in solar cells. The former is an II–VI semiconductor due to having direct band gap of 2.42 eV. This material together with narrow band gap materials such as CdTe, Cu$_2$S and InP has been used as a window layer [7, 8] in solar cell heterostructures [9, 10]. The latter is an important semiconductor among various potential metal oxides which are used as photocatalyst due to its chemical stability and commercial availability [11].These properties make TiO$_2$ as a potential n-type semiconductor. It is usually used as a powder in solution [6].

There are several deposition techniques to produce CdS thin films such as thermal evaporation [12], spray pyrolysis [13], laser evaporation [14], solid state reaction [10] and chemical bath deposition (CBD) [15, 16]. Among them, chemically deposited CdS thin film appears to be most suitable for solar cells application. However, this technique requires using ammonia, which is difficult to handle due to its volatility and relative toxicity, as a complexing agent for cadmium ions [17]. To overcome the problems, many researches have been conducted to ammonia-free synthesis of CdS [18–26]. In these researches, sodium citrate, ethylene diamine, etc. were used as an alternative to ammonia. Another approach to ammonia-free synthesis of CdS is the use of polymer for synthesizing semiconductor nanoparticles in thin film which provide the advantages such as (i) higher band gap, (ii) good adherence to the substrate and (iii) better coverage of the surface minimizing pin-holes and thereby permitting the use of very thin film of semiconductor (<100 nm) as a window layer in solar cell [27]. Life of the composites and their brightness of light emission are enhanced by the existence of semiconductor nanoparticles in polymeric matrices [28]. Nanocomposites impart several advantages such as greater chemical and thermal stability, increased strength, enhanced electrical conductivity, and improved flammability properties to polymeric matrix [29].There are many reports on the synthesis of semiconductor nanoparticles embedded into polymeric matrices [27, 28, 30–36].

Poly(vinyl alcohol) (PVA) is a semi-crystalline, hydrophilic polymer with good chemical and thermal stability [37]. PVA is highly biocompatible, non-toxic and water-soluble polymer that readily reacts with different cross-linking agents to form a gel [38, 39]. In addition, semi-crystalline PVA is greatly used as a polymeric matrix for preparation of nanocomposites by economically and environmentally friendly methods due to its easy processability and optical transparency [40–43].

The alternative method for preparing nanocomposite thin films is electrospinning. Immobilization of photocatalyst on nanofiber webs with the aim of increasing surface area for photocatalytic activity has been performed via electrospinning of photocatalyst contained polymer solution [6, 35]. Nanofibers obtained from electrospinning are very small in diameters which allow more chance for

nanoparticles to appear on fiber surface and as a result better exposure to radiation is accessible. This could provide enhanced photocatalytic activity.

In this work, we report the preparation of PVA/CdS and PVA/TiO$_2$ nanocomposite thin films at different ratio of semiconductor nanoparticles by employing electrospinning method. CdS nanoparticles are first synthesized using cadmium nitrate (Cd (NO$_3$)$_2$) and sodium sulphide (Na$_2$S) in a simple and economical way for preparation of PVA/CdS nanocomposites. In the case of PVA/TiO$_2$ nanocomposites, TiO$_2$ nanoparticles were purchased. Morphology and structure of nanocomposites are characterized by X-ray diffraction (XRD) and scanning electron microscopy (SEM). Optical properties of samples are characterized by diffuse reflectance spectroscopy (DRS). Finally, it is postulated that this method can yield pinhole free, homogeneous and transparent films which may be suitable for application as a window layer in solar cells.

Experimental part

Materials, instrumental and analysis methods

The chemicals used in the synthesis of all nanocomposites were obtained from Aldrich Chemicals and Merck Company and were used without further purification. Cd (NO$_3$)$_2$ (99 %) and Na$_2$S (35 %) were used as a source of cadmium ion and sulfide ion, respectively. TiO$_2$ nanoparticles (<15 nm) were purchased for preparation of PVA/TiO$_2$ thin layers. PVA with a weight average molecular weight (M_w) of 72,000 g/mol (97.5–99.5 mol% hydrolysis)was used as polymeric matrix for nanocomposites. SEM measurements were performed on a Philips XL30i. XRD measurements were taken using a Philips PW1840. DRS was measured using a Shimadzu UV–Vis 2100 spectrometer. Preparation of solution was carried out with Sonopuls ultrasonic homogenizer (Bandline HD 3100). Electrospinning of solutions was performed using a New era pump systems NE-1000.

Synthesis of CdS nanoparticles

0.3 M Cd (NO$_3$)$_2$ was stirred vigorously at ambient temperature for 30 min. 0.3 M Na$_2$S was added to adjust the pH of the solution in the range of 8–9. After 24 h, the sol was filtered and washed to remove all NaNO$_3$ and the water in the sol was replaced with absolute ethanol. The resulting alcogel was dried under vacuum at ambient temperature. The CdS in the form of gel was finally obtained.

Preparation of PVA/CdS and PVA/TiO$_2$ solutions

Aqueous PVA solution (10 wt%) was prepared by dissolving PVA in deionized (DI) water at 80 °C with constant stirring for at least 2 h. Aqueous solutions of CdS (10 wt%) and TiO$_2$ (10 wt%) were then prepared by dissolving CdS and TiO$_2$ nanoparticles powder in DI water, respectively, using ultrasonic homogenizer at room temperature. CdS solution at the following compositions; (v/v between CdS

and PVA ratio in DI) 20 (PVA/20CdS), 30 (PVA/30CdS), 40 (PVA/40CdS), and 50 (PVA/50CdS) was poured into a PVA solutions (pH = 6–7) to obtain PVA/CdS solutions. Also, PVA/TiO$_2$ solutions were prepared at different ratio of TiO$_2$ (20, 30, 40 and 50) as mentioned for PVA/CdS solutions.

Electrospinning of PVA/CdS and PVA/TiO$_2$ solutions

PVA/CdS and PVA/TiO$_2$ nanocomposite thin films were prepared using electro-spinning method. The electrospinning setup used in this research was composed of a high voltage DC power supply, a syringe with a flat-end needle (with inner diameter of 0.49 mm and length of 25 mm), a syringe pump and an electrically grounded aluminum plate. The solutions were electrospun with a constant feed rate of 0.2 μl min^{-1} at positive voltage of 10 kV at collection distance of 10 cm. The fibers were collected on the grounded aluminum plate. The electrospinning process was carried out at 30 °C and relative humidity of 60–70 %.

Results and discussion

Structural and surface morphology

The SEM images of PVA/CdS and PVA/TiO2 nanocomposite thin films are shown in Fig. 1. The appearance of semiconductor nanoparticles in PVA fibers clearly was increased by increasing the ratio of semiconductor. CdS and TiO$_2$ nanoparticles were well distributed in the PVA nano-fibrous matrix in both nanocomposites. No coagulation of the semiconductor nano-particles was observed in the matrix. This could be most likely attributed to the intermolecular interaction between the PVA solution and semiconductor nanoparticles and the strong electric field during electro-spinning. The average diameter of the both nanocomposites fibers was determined from SEM and is shown in Table 1. The diameter of the electrospun PVA/CdS and PVA/TiO2 fibers was found to decrease from 203 to 168 nm and 329 to 162 nm, respectively, as the ratio of CdS and TiO2 increased from 20 to 50. As the fiber diameter decreases, the surface area increases. From SEM images, it was found that the average diameter of both PVA/CdS and PVA/TiO$_2$ nanocomposite with 50:50 ratio is smaller than those of the other ratios, which can be interpreted as follows: thin layers with 50:50 ratio had a higher surface area than the others. Therefore, high concentration of semiconductor nanoparticles in the nanofiber resulted in a high active surface area which actually enhanced the photocatalytic activity [6]. Also, the particles' size was determined by XRD analysis and absorption spectra which were in agreement with each other.

XRD results indicated the cubic and anatase phase of CdS and TiO$_2$ nanoparticles formed within the pores of PVA matrix, respectively. The results show the influence of CdS and TiO$_2$ nanoparticles upon the crystalline structure of PVA. Figure 2 shows the X-ray diffraction spectra of PVA/CdS nanocomposite thin films prepared at different ratios. The X-ray diffractogram of PVA/CdS nanocomposites shows broadened diffraction profiles. The peaks were detected at around $2\theta = 26.5°$ and
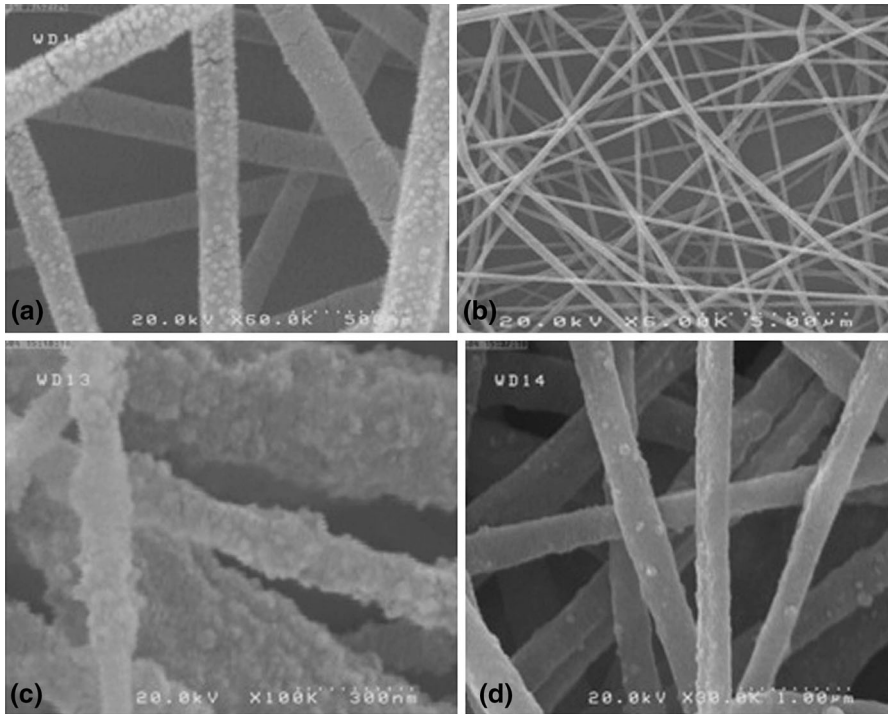
Fig. 1 SEM images of distribution of nanoparticles in PVA matrix for **a** PVA/CdS, 50:50; **b** PVA/CdS, 80:20; **c** PVA/TiO2, 50:50; **d** PVA/TiO2, 80:20 ratio

Table 1 Diameter of PVA/CdS and PVA/TiO$_2$ nano fibers from SEM	Ratio	Average diameter of fibers (nm)	
		PVA/CdS	PVA/TiO$_2$
	80:20	203	329
	70:30	189	269
	60:40	178	234
	50:50	168	162

43.3° which can be ascribed due to the cubic CdS structure [27, 44, 45]. These peaks can be indexed to the planes (111) and (220) [46].

The X-ray diffraction spectra of PVA/TiO$_2$ nanocomposite thin films are shown in Fig. 3. The peaks at around $2\theta = 25.47°$, 38° and 47.9° show the anatase structure of TiO$_2$ nanoparticles in PVA matrix. It is known that the crystalline nature of PVA results from the strong intermolecular interaction between PVA chains through the intermolecular hydrogen bonding. By comparing the X-ray diffraction patterns for PVA/CdS and PVA/TiO$_2$ nanocomposite, it can be noticed that there is a noticeable change in the intensity of XRD peaks which become
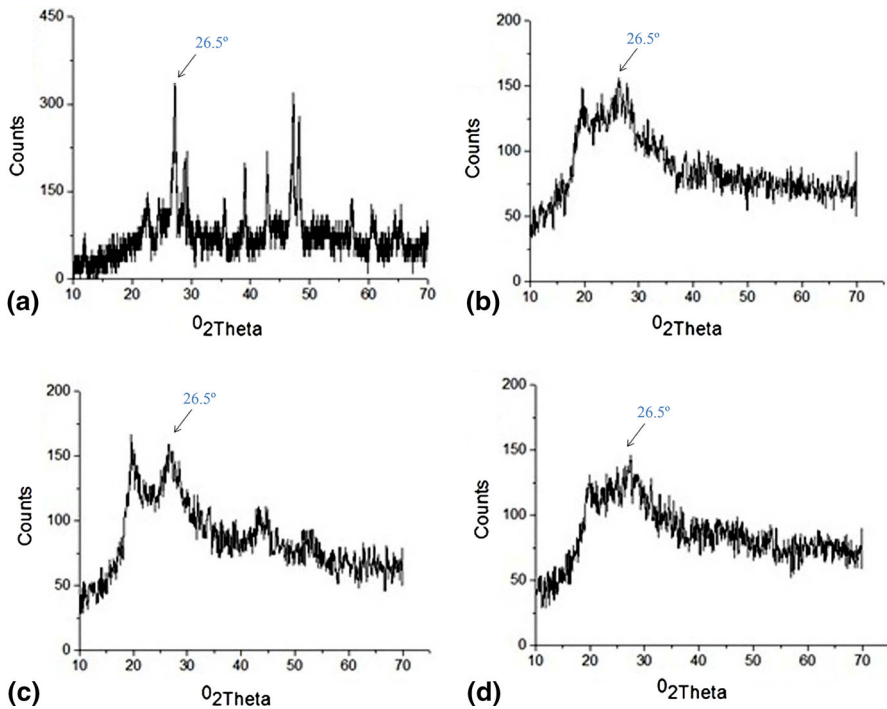
Fig. 2 XRD patterns of PVA/CdS at different CdS ratio: **a** 50; **b** 40; **c** 30 and **d** 20

weaker and broader with decreasing the volume ratio of semiconductors nanoparticles. Also, the weak intensity and broad diffraction peak at around ($2\theta = 20°$) indicates the absence of crystalline phase of the PVA. This behavior can be correlated to the intermolecular interactions between PVA and CdS and TiO$_2$ nanoparticles, respectively. Thus, it is possible that in our study the interactions between PVA chains and semiconductor particles led to the decrease of intermolecular interaction between the PVA chains and thus the crystalline degree decreases. The particle size of the semiconductors in thin films is estimated using the Scherrer formula, Eq. (1) [46–49].

$$D = K\lambda / \beta_{2\theta} \cos \theta \qquad (1)$$

where K is a constant taken to be 0.94, λ the wavelength of X-ray used ($\lambda = 1.54$ Å) and $\beta_{2\theta}$ the full width at half maximum of diffraction peak of XRD pattern, Bragg angle 2θ, is around 26.5° and 25.47° for CdS and TiO$_2$, respectively. The values of particle sizes of the films are shown in Table 2. The particle sizes of CdS and TiO$_2$ nanoparticles were found to be in agreement with the results obtained from EMA method and absorption spectra. The prominent peaks seen in Figs. 2a and 3a for the case of the film synthesized at 50:50 ratio are indication of good crystallinity of the film for both PVA/CdS and PVA/TiO$_2$ nanocomposites.
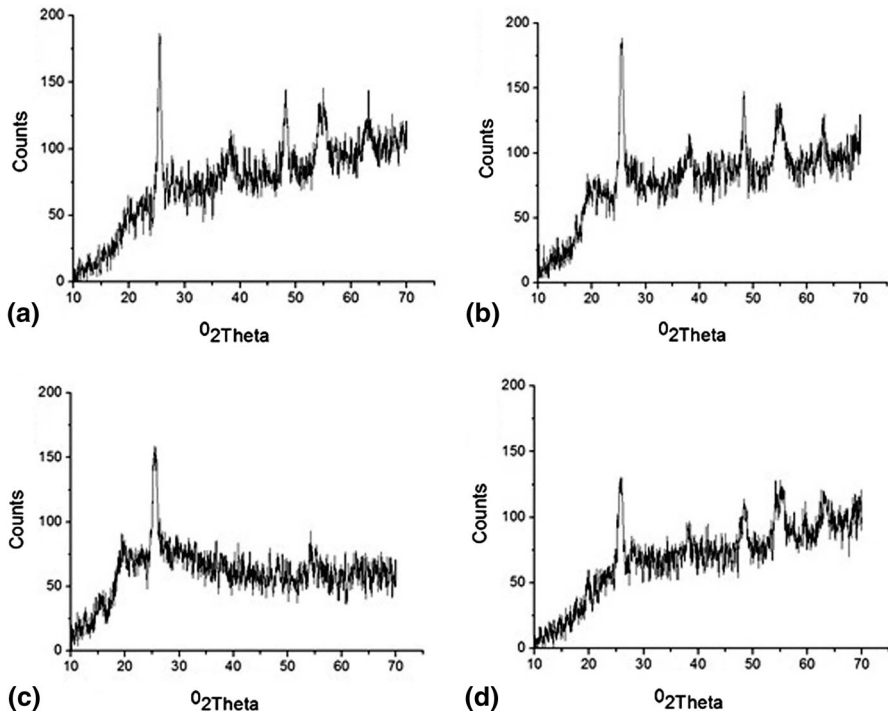
Fig. 3 XRD patterns of PVA/TiO$_2$ at different TiO$_2$ ratio: **a** 50; **b** 40; **c** 30 and **d** 20

Table 2 Particle sizes calculated from Scherrer fomula (XRD)

Ratio	Particle size (nm)	
	PVA/CdS	PVA/TiO$_2$
80:20	5.86	9.14
70:30	6.26	10.56
60:40	7.12	12.43
50:50	7.89	13.16

Absorption spectra of the PVA/CdS and PVA/TiO$_2$ nanocomposites

Optical properties which are directly related to the size of nanoparticles can be studied using the absorption spectra of nanocomposites. The UV–Vis absorption spectra of the PVA/CdS and PVA/TiO$_2$ nanocomposite thin films prepared at various semiconductor ratios (20, 30, 40 and 50) are shown in Fig. 4. It is evident from the spectra that absorbance edges of all the films are blue shifted relative to the bulk CdS (520 nm) and bulk TiO$_2$ (388 nm) indicating quantum confinement effect in nanoparticles [27, 50]. Optical properties of semiconductor nanoparticles are dependent on the size of particles which render them attractive from the viewpoint of integrated photonic devices. Optical properties are changed considerably by the
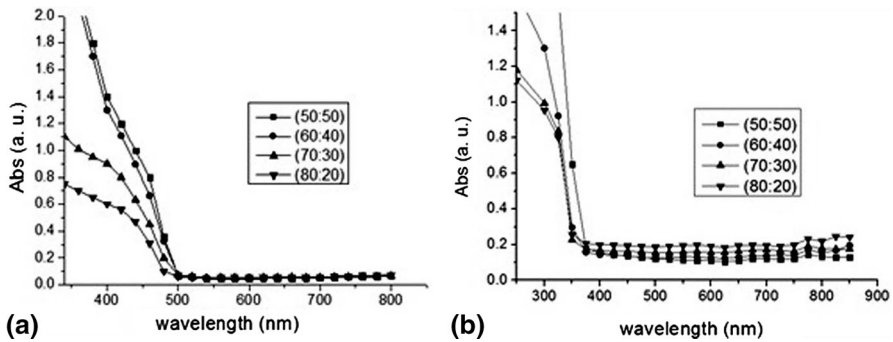
Fig. 4 UV–Vis absorption spectra of **a** PVA/CdS; **b** PVA/TiO$_2$ nanocomposite thin films

Table 3 Band gap, shift in band gap and particle sizes calculated from absorption spectra

Ratio	PVA/CdS			PVA/TiO$_2$
	Band gap from UV–Vis (eV)	Shift in band gap (eV)	Grain size from EMA (nm)	Band gap (eV)
80:20	2.62	0.2	6.1	3.51
70:30	2.60	0.18	6.43	3.49
60:40	2.56	0.14	7.3	3.46
50:50	2.53	0.11	8.22	3.31

dimensions of the nanocrystallites when they are comparable or less than Bohr radius of exciton wave function. In molecular terminology, this refers to the broadening of the energy gap as size decreases [51]. In Fig. 4, the sharp increase in absorbance near the absorption edge for the films prepared at 50:50 ratio, for both nanocomposites, is an indication of good crystallinity of the nanostructures inside the matrix. A little redshift in absorption edges among the spectra was observed as the nanoparticle ratio was increased from 20 to 50. In contrast, when the proportion of nanoparticle is low, a well-defined blue shift was observed indicating good quantum confinement. However, although the crystallinity of sample with the proportion of 50:50 was high according to XRD characterization, the absorption edge was not sharp compared with the absorption edge of the other samples and this is in agreement with the finding of other researchers [27]. The decrease in particle sizes of the films with the reduction in CdS ratio in PVA/CdS nanocomposites, calculated by effective mass approximation (EMA) method, could be the reason of observed blue shift. A summary of the results of the absorption spectroscopy measurements is shown in Table 3.

According to Thambidurai et al. definition [51], there are two situations, called the weak confinement and the strong confinement regime. In the weak regime, the particle radius is larger than the radius of the electron–hole pair, but the range of motion of the exciton is limited, which causes a blue shift of the absorption spectrum. When the radius of the particle is smaller than the orbital radius of the

electron–hole pair, the motion of electron and hole become independent and the exciton does not exist. The hole and the electron have their own set of energy levels. Here also there is a blue shift. As the particle size obtained from optical absorption studies is larger than the Bohr radius of 3 nm for both CdS and TiO$_2$, the weak confinement effect can be assumed to be present in the mentioned nanoparticles.

Transmittance spectra of the PVA/CdS and PVA/TiO$_2$ nanocomposites

Figure 5 shows the transmission versus wavelength plot of PVA/CdS and PVA/TiO$_2$ nanocomposite thin films prepared at different ratio. It is evident from the spectra that all the films show high transmittance for wavelength greater than 500 nm. However, a little higher transmittance ($\sim$90 % for PVA/CdS and $\sim$80 % for PVA/TiO$_2$) was observed for the film, which was prepared at 50:50 ratio for both nanocomposites. The sharp fall in transmission near the fundamental absorption edge shows good crystallinity of the film [28].

Optical band gap of the PVA/CdS and PVA/TiO$_2$ nanocomposites

The optical band gaps of the films were obtained using Eq. (2) [52] for a semiconductor

$$A = \frac{K(hv - E_g)^{m/2}}{hv} \tag{2}$$

where 'A', 'K', 'E_g' and 'hv' are the absorbance, constant, band gap of the semiconductor and incident photon energy, respectively, and 'm' is equal to '1' for direct transition and '2' for indirect transition. According to linear plot of $(Ahv)2$-hv for nanocomposite thin films, 'm' is equal to '1'. Band gap of the film material is obtained by extrapolation of the straight line to $(Ahv)2 = 0$ axis (Fig. 6). The band gap of the PVA/CdS films was found to gradually increase from 2.53 to 2.62 eV as the CdS ratio was reduced from 50 to 20 and the band gap of the PVA/TiO2 films increased from 3.31 to 3.51 eV with the reduction of TiO2 ratio, too (Table 3). The
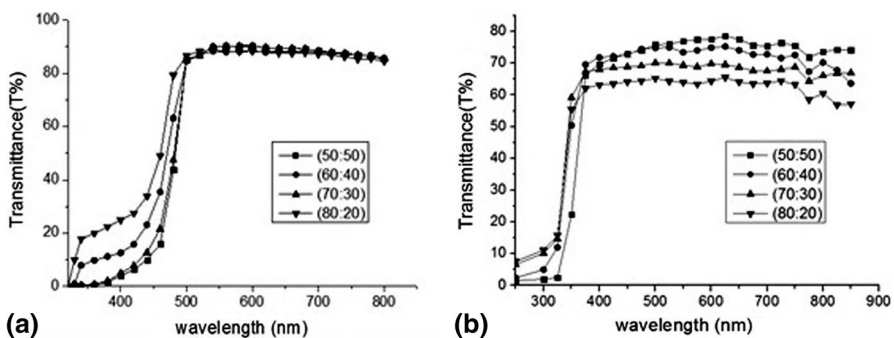

Fig. 5 Transmittance spectra of **a** PVA/CdS; **b** PVA/TiO$_2$ nanocomposite thin films
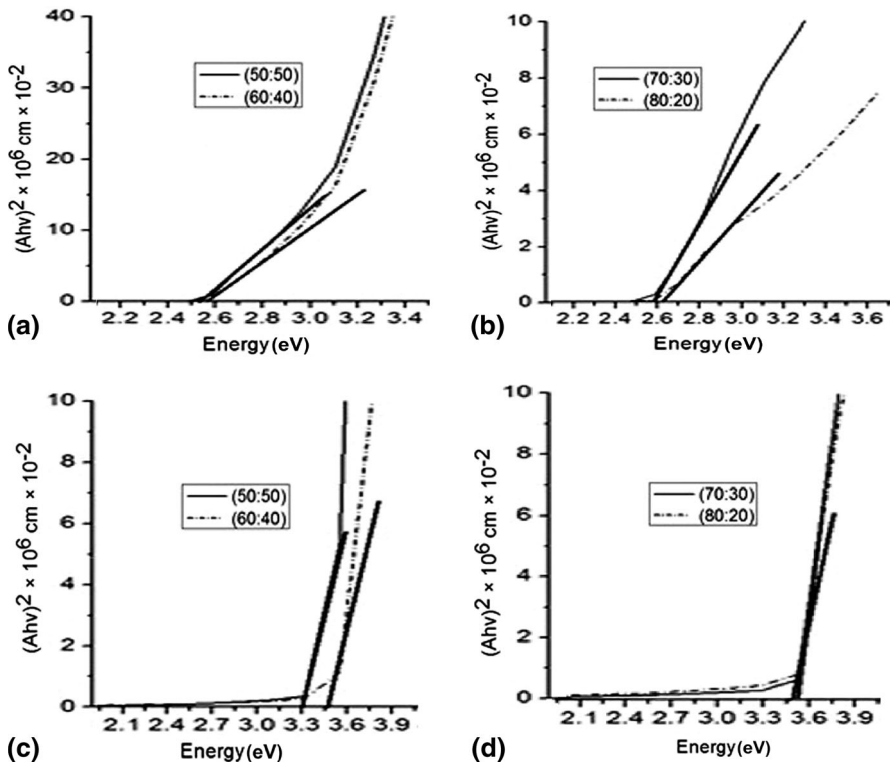
Fig. 6 Band gap spectra of **a** PVA/CdS, 50:50 and 60:40; **b** PVA/CdS, 70:30 and 80:20; **c** PVA/TiO$_2$, 50:50 and 60:40; **d** PVA/TiO$_2$, 70:30 and 80:20

size of the CdS nanoparticles was calculated by the use of EMA method and Eq. (3) for a semiconductor [44, 52].

$$E_{gn} - E_{gb} = \frac{(h^2\pi^2/2R^2)1}{m^*} \tag{3}$$

where m^* is the effective mass of the specimen, R is radius of the particle, E_{gb} is the bulk band gap and E_{gn} is the band gap of the sample. From the calculations, it is found that the particle size decreases with the reduction in CdS ratio. The observations are shown in Table 3 and CdS particle sizes were in the range of 6.1–8.22 nm.

Conclusion

PVA/CdS and PVA/TiO$_2$ nanocomposite thin films were prepared by means of electrospinning method. This production method is simple, low cost and helps increasing semiconductor nanoparticles photocatalytic activity. XRD results

indicated the cubic and anatase phase of CdS and TiO_2 nanoparticles formed within the pores of PVA matrix, respectively. The blue shift in the absorbance spectra was attributed to the quantum confinement effect in nanoparticles. The film prepared at 50:50 ratio showed better optical and structural properties in comparison to the films prepared at lower semiconductor ratio for both nanocomposites. SEM analysis showed that semiconductor nanoparticles were successfully coated by polyvinyl alcohol molecules. The particle sizes obtained from XRD analysis were in good agreement with the results obtained from absorption spectra. The film prepared at 50:50 ratio for both PVA/CdS and PVA/TiO_2 is more suitable for application as a window layer in solar cell because of its favorable optical band gap (2.53, 3.31 eV), high transmittance and good crystallinity.

References

1. Britt J, Ferekids C (1993) Thin- film CdS- CdTe solar cell with 15.8 % efficiency. Appl Phys Lett 62:2851–2852
2. Danaher WA, Lyons LE, Morris GC (1985) Some properties of thin films of chemically deposited cadmium sulphide. Sol Energy Mater 12:137–148
3. Kashiwaba Y, Sato J, Abe T (2003) Emission of lights of various colors from p-CdS:Cu/n-CdS thin-film diodes. Appl Surf Sci 212–213:162–165
4. Senthil K, Mangalraj D, Narayandass SK (2001) Structural and optical properties of CdS thin films. Appl Surf Sci 169–170:476–479
5. Ullrich B, Bangall DM, Sakai H, Segawa Y (2000) Photoluminescence and lasing of thin CdS films on glass formed by pulsed-laser-deposition. J Lumin 87–89:1162–1164
6. Linh BNT, Lee KH, Lee BT (2011) Fabrication of photocatalytic PVA-TiO_2 nano fibrous hybrid membrane using the electrospinning method. J Mater Sci 46:5615–5620
7. Su B, Choy KL (2000) Microstructure and properties of the CdS thin films prepared by electrostatic spray assisted vapour deposition (ESAVD) method. Thin Solid Films 359:160–164
8. Mahmoud SA, Ibrahim AA, Raid AS (2000) Physical properties of thermal coating CdS thin films using a modified evaporation source. Thin Solid Films 372:144–148
9. Romeo A, Batzner DL, Zoog H, Vignali C, Tiwari AN (2001) Influence of CdS growth process on structural and photovoltaic properties of CdTe/CdS solar cells. Sol Energy Mater Sol Cells 67:311–321
10. Kylner A (1999) Effect of impurities in the CdS buffer layer on the performance of the $Cu(In, Ga)Se_2$ thin film solar cell. J Appl Phys 85:6858–6865
11. Fujishima A, Zhang X (2006) Titanium dioxide photocatalysis: present situation and future approaches. C R Chim 9:750–760
12. Castillo SJ, Mendoza-Galvan A, Ramirez-Bon R, Espinoza-Beltran FJ, Sotelo-Lerma M, Gonzalez-Hernandez J, Martinez G (2000) Structural, optical and electrical characterization of In/CdS/glass thermally annealed system. Thin Solid Films 373:10–14
13. Wang XW, Spitulnik F, Campell B, Noble R, Hapanowicz RP, Condrate Sr RA, Fu LP, Peteou A (1992) Continous wave Nd:YAG laser deposition of CdS thin films. Thin Solid Films 218:157–160
14. Choy KL, Su B (2001) Growth behavior and microstructure of CdS thin films deposited by an electrostatic spray assisted vapor deposition (ESAVD) process. Thin Solid Films 388:9–14
15. Rakhshani E, Al-Azab AS (2000) Characterization of CdS films prepared by chemical-bath deposition. J Phys Condens Matter. 12:8745–8755
16. Sasikala G, Thilakan P, Subramanian C (2000) Modification in the chemical bath deposition apparatus, growth and characterization of CdS semiconducting thin films for photovoltaic applications. Sol Energy Mater Sol Cells 62:275–293

17. Archbold MD, Halliday DP, Durose K, Hase TPA, Boyle DS, Mazzamuto S, Romeo N, Bosio A (2007) Development of low temperature approaches to device quality CdS: a modified geometry for solution growth of thin films and their characterization. Thin Solid Films 515:2954–2957

18. Sandoval-Paz MG, Sotelo-Lerma M, Mendoza-Galvan A, Ramirez-Bon R (2007) Optical properties and layer microstructure of CdS films obtained from an ammonia-free chemical bath deposition process. Thin Solid Films 515:3356–3362

19. Mazon-Montijo DA, Sotelo-Lerma M, Qudevo-Lopez M, El-Bouanani M, Alshareef HN, Espinoza-Beltran FJ, Ramirez-Bon R (2007) Morphological and chemical study of the initial growth of CdS thin films deposited using an ammonia-free chemical process. Appl Surf Sci 254:499–505

20. Elashmawi IS, Hakeem NA, Selim MS (2009) Optimization and spectroscopic studies of CdS/poly(vinyl alcohol) nanocomposites. Mater Chem Phys 115:132–135

21. Zhang H, Ma X, Yang D (2004) Effects of complexing agent on CdS thin films prepared by chemical bath deposition. Mater Lett 58:5–9

22. Ortuno-Lopez MB, Sotelo-Lerma M, Mendoza-Galvan A, Ramirez-Bon R (2004) Chemically deposited CdS films in an ammonia-free cadmium–sodium citrate system. Thin Solid Films 457:278–284

23. Nemec P, Nemec I, Nahalkova P, Nemcova Y, Trojanek F, Maly P (2002) Ammonia-free method for preparation of CdS nanocrystalline films by chemical bath deposition technique. Thin Solid Films 403:9–12

24. Boyle DS, Bayer A, Heinrich MR, Robbe O, O'Brien P (2000) Novel approach to the chemical bath deposition of chalcogenide semiconductors. Thin Solid Films 361:150–154

25. Feitosa AV, Miranda MAR, Sasaki JM, Araujo-Silva MA (2004) A new route for preparing CdS thin films by chemical bath deposition using EDTA as ligand. Braz J Phys 34:656–658

26. Kanade KG, Hawaldar RR, Pasricha R, Radhakrishan S, Seth T, Mulik UP, Kale BB, Amalnerkar DP (2005) Novel polymer-inorganic solid-state reaction for the synthesis of CdS nanocrystallites. Mater Lett 59:554–559

27. Saika D, Saika PK, Gogoi PK, Das MR, Sengupta P, Shelka MV (2011) Synthesis and characterization of CdS/PVA nano composite thin films from a complexing agent free system. Mater Chem Phys 131:223–229

28. Khanna P, Gokhale RR, Subbarao VVVS, Singh N, Jun KW, Das BK (2005) Synthesis and optical properties of CdS/PVA nano composites. Mater Chem Phys 94:454–459

29. Radoicic MB, Saponjic ZV, Marinovic-Cincovic MT, Ahrenkiel SP, Bibic NM, Nedeljkovic JM (2011) The influence of shaped TiO_2 nanofillers on the thermal properties of poly(vinyl alcohol). J Serb Chem Soc 76:1–3

30. Han Z, Zhang J, Yang X, Coa W (2011) Synthesis and application in solar cell of (3-Octylthiophene)/cadmium sulfide nano composite. Sol Energy Mater Sol Cells 95:483–490

31. Firth AV, Haggata SW, Khanna PK, Williams SJ, Allen JW, Magennis SW, Samuel IDW, Cole-Hamilton DJ (2004) Production and luminescent properties of CdSe and CdS nanoparticle-polymer composites. J Lumin 109:163–172

32. Lee J, Sundar VC, Heine JR, Bawendi MG, Jensen KF (2000) Full color emission from II–VI semiconductor quantum dot-polymer composites. Adv Mater 12:1102–1105

33. Qi L, Colfen H, Antonietti M (2001) Synthesis and characterization of CdS nanoparticles stabilized by double-hydrophilic block copolymers. Nano Lett 1:61–65

34. Zhan J, Yang X, Wang D, Li S, Xie Y, Xia Y, Qian Y (2000) Polymer-controlled growth of CdS nanowires. Adv Mater 12:1348–1351

35. Prahsarn C, Klinsukhon W, Roungpaisan N (2011) Electrospinning of PAN/DMF/H_2O containing TiO_2 and photocatalytic activity of their webs. Mater Lett 65:2498–2501

36. Maurya A, Chauhan P (2012) Synthesis and characterization of sol–gel derived PVA-titanium dioxide (TiO_2) nanocomposite. Polym Bull 68:961–972

37. Shao C, Kim HY, Gong J, Ding B, Lee D, Park S (2003) Fiber mats of poly(vinyl alcohol)/silica composite via electrospinning. Mater Lett 57:1579–1584

38. Krumova M, Lopez D, Benavente R, Mijangos C, Perena JM (2000) Effect of crosslinking on the mechanical and thermal properties of poly(vinyl alcohol). Polymer 41:9265–9272

39. Hodge RM, Edward GH, Simon GP (1996) Water absorption and states of water in semicrystalline poly(vinyl alcohol) films. Polymer 37:1371–1376

40. Li Y, Neoh KG, Kan ET (2004) Poly (vinyl alcohol) hydrogel fixation on poly (ethylene terephthalate) surface for biomedical application. Polymer 45:8779–8789

41. Kuljanin J, Comor MI, Djokovic V, Nedeljkovic JM (2006) Synthesis and characterization of nanocomposite of polyvinyl alcohol and lead sulfide nanoparticles. Mater Chem Phys 95:67–71
42. Liu L, Qi Z, Zhu X (1999) Studies on nylon 6/clay nanocomposites by melt-intercalation process. J Appl Polym Sci 71:1133–1138
43. Kuljanin-Jakovljevic J, Stojanovic Z, Nedeljkovic JM (2006) Influence of CdS-filler on the thermal properties of poly (methyl methacrylate). J Mater Sci 41:5014–5016
44. Siakia D, Siakia PK, Gogoi PK, Siakia P (2011) Synthesis, characterization and photovoltaic application of silver doped CdS/PVA nanocomposite thin films. Dig J Nanomater Bios 6:589–597
45. Devi R, Purkayastha P, Kalita PK, Sarma BK (2007) Synthesis of nanocrystalline CdS thin films in PVA matrix. Bull Mater Sci 30:123–128
46. Seoudi R, El- Bailly AB, Eisa W, Shabaka AA, Soliman SI, Abd El Hamid RK, Ramadan RA (2012) Synthesis, optical and dielectric properties of (PVA/CdS) nanocomposites. J Appl Sci Res 8:658–667
47. Kawar SS, Pawar BH (2009) Synthesis and characterization of CdS n-type of semiconductor thin films having nanometer grain size. Chalcogenide Lett 6:219–225
48. Dumbrava A, Badea C, Prodan G, Ciupina V (2010) Synthesis and characterization of cadmium sulfide obtained at room temperature. Chalcogenide Lett 7:111–118
49. Prabhu RR, Khadar MA (2005) Characterization of chemically synthesized CdS nanoparticles. Pramana J Phys 65:801–807
50. Hua MA, De-Yong SU, Wei XU, Feng GAO, Jun CHEN (2006) CdS microspheres: hydrothermal synthesis and UV–Vis spectroscopy. Chin J Inorg Chem 22:83–86
51. Thambidurai M, Muthukumarasamy N, Agilan S, Murugan N, Vasantha S, Balasundaraprabhu R, Senthil TS (2010) Strong quantum confinement effect in nanocrystalline CdS. J Mater Sci 45:3254–3258
52. Subramanian B, Sanjeeviraja C, Jayachandran M (2002) Brush plating of tin(II) selenide thin films. J Cryst Growth 234:421–426